

Reactivity and Properties of $[-O-Bi^{III}\cdots O=Mo-]_n$ ChainsStefan Roggan,[†] Christian Limberg,^{*,†} Burkhard Ziemer,[†] Maike Siemons,[‡] and Ulrich Simon^{*,‡}*Humboldt-Universität zu Berlin, Institut für Chemie, Brook-Taylor-Strasse 2, 12489 Berlin, Germany, and RWTH Aachen, Institut für Anorganische Chemie, Landoltweg 1, 52056 Aachen, Germany*

Received June 30, 2006

A coordination polymer $[Cp^*(O)_2Mo-O-Bi(o\text{-tolyl})_2]_n$, **II**, containing $Mo-O-Bi$ and $Mo=O\cdots Bi$ moieties was investigated with respect to its behavior in contact with OH^- and Cp_2MoH_2 and as potential single source precursor in the polyol method. It turned out that hydroxide as a base breaks up the polymer to yield $Cp^*MoO_3^-$ and $(o\text{-tolyl})_2BiOH$. The latter polymerizes to give the coordination polymer $[(o\text{-tolyl})_2BiOH]_n$, **1**. Alternatively, **1** can be prepared by reacting $[(o\text{-tolyl})_2Bi(hmpa)_2]SO_3CF_3$ with NBu_4OH/H_2O in $thf/water$. If, however, $NBu_4OH/MeOH$ is used in dichloromethane as the solvent, the $(o\text{-tolyl})_2BiOH$ formed intermediately undergoes methanolysis, and finally, $[(o\text{-tolyl})_2BiOMe]_n$, **3**, is isolated. Although **1** and **3** are very similar compounds, their crystal structures differ significantly: while the structure of **1** is dominated by secondary bonding leading to seesaw-type coordination geometries around the Bi centers, the Bi atoms in **3** are coordinated in a distorted tetrahedral fashion, and secondary bonding plays only a minor role. If **1** is dissolved in a nonpolar, nonprotic solvent, condensation reactions occur immediately leading to $[(o\text{-tolyl})_2BiOBi(o\text{-tolyl})_2]$, **2**, which can be obtained on a preparative scale this way. Compound **3** which can be prepared in good yields may prove to be a useful starting material in bismuth chemistry. Here, it was shown to react with molybdocene dihydrides to provide stable Bi-substituted molybdocene monohydrides $[^R Cp_2Mo(H)(Bi(o\text{-tolyl})_2)]$ ($R = Me$ **4**, $R = H$ **5**); compounds of that type were identified in solution before but had so far eluded isolation. Compound **4**, whose crystal structure is discussed, also forms when **II** is treated with methylated molybdocene dihydride. This obviously leads to the formation of $Mo-Bi$ bonds (\rightarrow **4**), as well as $Mo-OH$ units, which undergo condensation reactions leading to $Mo-O-Mo$ moieties (i.e., $[Cp^*_2Mo_2O_5]$ is formed as a byproduct). The use of **II** as precursor in the polyol method successfully led to bismuthmolybdate nanoparticles (accompanied by crystallites); however, no single phase is obtained, but biphasic materials consisting of $Bi_2Mo_2O_9$ and Bi_2MoO_6 , whose ratio can be determined by the choice of the hydrolyzing reagent, are formed instead. One of these materials proved to be capable of sensing EtOH selectively at elevated temperatures.

Introduction

$nMoO_3/Bi_2O_3$ phases represent heterogeneous catalysts for the allylic oxidation of propene. The reasons why exactly this combination of metals is most efficient are still discussed controversially.¹ The favorable properties of bismuthmolybdates might be related inter alia to the presence of $Mo-O-Bi$ linkages on the surface of these solids, assuming that such assemblies possess favorable H abstraction or radical trapping properties.^{1g,h} This hypothesis naturally stimulates attempts aimed at establishing $Mo-O-Bi$ units in molecular compounds also. However, no structurally characterized molec-

ular $Mo-O-Bi$ complexes existed in the literature until recently, when we achieved the synthesis and isolation of such complexes containing Bi atoms in oxidation states +III and +V (see Chart 1).² Here, we describe the results of an investigation concerning the reactivity and properties of one of these compounds, the coordination polymer **II**.

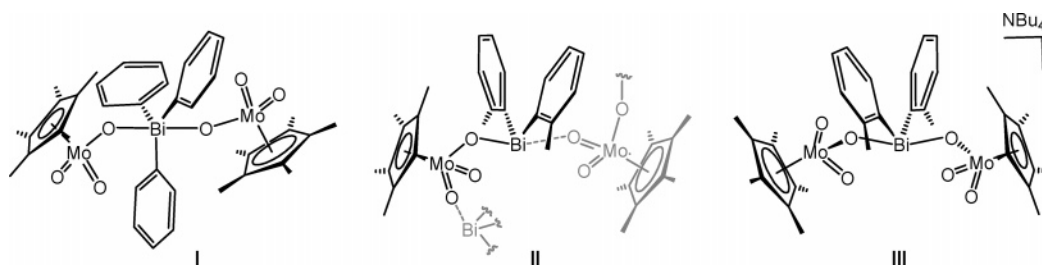
* To whom correspondence should be addressed. E-mail Christian.limberg@chemie.hu-berlin.de (C.L.); ulrich.simon@ac.rwth-aachen.de (U.S.).

[†] Humboldt-Universität zu Berlin.

[‡] RWTH Aachen.

(1) (a) Keulks, G. W.; Krenzke, L. D.; Notermann, T. M. *Adv. Catal.* **1978**, *27*, 183. (b) Grasselli, R. K.; Burrington, J. D. *Adv. Catal.* **1981**, *30*, 133. (c) Grasselli, R. K.; Burrington, J. D. *Ind. Eng. Chem. Prod. Res. Dev.* **1984**, *23*, 393. (d) Belagem, J.; Osborn, J. A.; Kress, J. J. *Mol. Catal.* **1994**, *86*, 267. (e) Grasselli, R. K. In *Handbook of Heterogeneous Catalysis*; Ertl, G., Knözinger, H., Weitkamp, J., Eds.; VCH Verlagsgesellschaft mbH: Weinheim, Germany, 1997; p 2302. (f) Jang, Y. H.; Goddard, W. A., III. *Top. Catal.* **2001**, *15*, 273. (g) Limberg, C. *Angew. Chem.* **2003**, *115*, 6112; *Angew. Chem., Int. Ed.* **2003**, *42*, 5932. (h) Hanna, T. A. *Coord. Chem. Rev.* **2004**, *248*, 429 and references therein.

Chart 1



Experimental Section

General Procedures. All manipulations were carried out in a glovebox or with Schlenk-type techniques with a dry argon atmosphere. The ¹H and ¹³C{¹H} NMR spectra were recorded on a Bruker AV 400 NMR spectrometer (¹H, 400.13 MHz; ¹³C, 100.61 MHz) with C₆D₆ and CD₂Cl₂ as the solvents at 22 °C. The ¹H and ¹³C{¹H} NMR spectra were calibrated against the residual proton and natural abundance ¹³C resonances of the deuterated solvent (benzene-*d*₆, δ_H 7.15 and δ_C 128.02; dichloromethane-*d*₂, δ_H 5.32 and δ_C 53.5). Microanalyses were performed on a Leco CHNS-932 elemental analyzer. Infrared (IR) spectra were recorded using samples prepared as KBr pellets with a Digilab Excalibur FTS 4000 FTIR spectrometer. The powder morphology was examined by SEM analysis using a LEO Supra 35VP equipped with an EDX system (Inca Energy 200, Oxford, U.K.). For that purpose, all samples were coated with carbon. Conductivity measurements were performed with an Agilent 4192 A impedance analyzer. Electrical characterization was performed using a Keithley 2400 source meter and an Agilent 4192 A (for response measurements).

Materials. Solvents were purified, dried, and degassed prior to use. [(*o*-Tolyl)₂Bi(OTf)(hmpa)₂] (hmpa = hexamethylphosphoramide),³ [Cp₂MoH₂],⁴ and [MeCp₂MoH₂]⁵ were prepared according to the literature procedures. (*n*-C₄H₉)₄NOH (a 1 M solution in methanol or a 40% solution in water) was obtained commercially and used as received.

[(*o*-Tolyl)₂BiOH]_∞, **1**. A 7.25 g portion of a 40% solution of (*n*-C₄H₉)₄NOH in H₂O (11.1 mmol) was diluted with an additional 60 mL of H₂O and then added to a solution of 2 g (2.2 mmol) of [(*o*-tolyl)₂Bi(OTf)(hmpa)₂] in 20 mL of THF. A colorless solid precipitated, which was filtered off after the suspension had been stirred for 1 h at room temperature. The residue was washed with water and diethyl ether. Finally, it was dried in vacuo to yield 591 mg (1.45 mmol, 65%) of a crude product, which was shown by IR spectroscopy and elemental analysis to consist mainly of **1**. Analytically pure samples can be obtained by recrystallization from ethanol (96%, used as received). Anal. Calcd for C₁₄H₁₅BiO: C, 41.19; H, 3.70. Found: C, 41.04; H, 3.63. IR (KBr, cm⁻¹): ν̄ 3617 m, 3065 w, 3045 m, 2992 w, 2961 w, 2950 w, 2917 w, 2856 w, 1579 w, 1560 w, 1445 br, 1376 w, 1265 m, 1197 m, 1157 w, 1116 w, 1043 w, 1029 w, 938 w, 858 w, 834 s, 790 m, 737 s, 707 w, 644 w, 540 m, 486 m, 425 m.

[(*o*-Tolyl)₂BiOBi(*o*-tolyl)₂], **2**. A 40% solution of (*n*-C₄H₉)₄NOH in H₂O (0.72 mL, 1.1 mmol) was added dropwise to a solution of 1.0 g (1.1 mmol) of [(*o*-tolyl)₂Bi(OTf)(hmpa)₂] in 10 mL of acetone.

A white precipitate formed, and the suspension was stirred for 2 h at room temperature. Concentration and filtration yielded a white solid consisting of **1** and **2** (according to IR analysis), which was washed with acetone and dried in vacuo. The solid was redissolved in CH₂Cl₂, and the resulting solution was stirred for 10 min at room temperature. Subsequently, all volatiles were removed to yield a bright yellow powder (320 mg, 73%), which was shown to consist solely of **2** by means of IR spectroscopy. Analytically pure samples can be obtained by recrystallization from THF or toluene. Anal. Calcd for C₂₈H₂₈Bi₂O: C, 42.12; H, 3.53. Found: C, 42.52; H, 3.60. ¹H NMR (CDCl₃): δ 8.20 (d, 4H CH), 7.40 (t, 4H CH), 7.31 (d, 4H CH), 7.24 (t, 4H CH), 2.15 (s, 12H *o*-CH₃) (in agreement with ref 6a). ¹³C{¹H} NMR (CDCl₃): δ 181.4/143.2/135.6/131.3/128.9/128.3 (C_{Ar}), 23.9 (*o*-CH₃). IR (KBr, cm⁻¹): ν̄ 3052 m, 3039 m, 3026 m, 2991 w, 2966 m, 2933 w, 2912 w, 2854 w, 1578 m, 1562 w, 1444 s, 1374 m, 1277 w, 1266 m, 1201 s, 1153 m, 1112 m, 1043 m, 1030 m, 1017 m, 984 w, 951 w, 943 w, 870 w, 792 m, 744 vs, 618 vs, 535 w, 484 w 426 s.

[(*o*-Tolyl)₂BiOCH₃]_∞, **3**. A 1 M solution (0.9 mL) of (*n*-C₄H₉)₄NOH in CH₃OH (0.9 mmol) was added to a solution of 809 mg (0.9 mmol) of [(*o*-tolyl)₂Bi(OTf)(hmpa)₂] in 10 mL of CH₂Cl₂. A turbid solution formed, which was stirred for 2 h at room temperature and filtered. The filtrate was concentrated until a white precipitate began to form. After the addition of a minimum amount of CH₂Cl₂ to redissolve the precipitate, the clear solution was cooled to −30 °C. After a few days, a white precipitate had formed, which was filtered off and dried in vacuo to yield 0.262 mg (0.62 mmol, 69%) of **3**. ¹H NMR spectroscopic data revealed a contamination by small amounts of the condensation product [(*o*-tolyl)₂BiOBi(*o*-tolyl)₂], **2**, which can be separated by recrystallization from CH₂Cl₂ at −30 °C. The first fraction of the crystallization is purer when 5 mL of MeOH are added to the initial solution of [(*o*-tolyl)₂Bi(OTf)(hmpa)₂] in CH₂Cl₂. Anal. Calcd for C₁₅H₁₇BiO: C, 42.66; H, 4.06. Found: C, 42.41; H, 3.93. ¹H NMR (C₆D₆): δ 8.38 (d, 2H CH), 7.30 (t, 2H CH), 7.19 (d, 2H CH), 7.09 (t, 2H CH), 4.23 (s, 3H OCH₃), 2.11 (s, 6H *o*-CH₃). ¹³C{¹H} NMR (C₆D₆): δ 143.5 (*o*-CCH₃), 135.9/132.0/129.4/128.8 (CH), 57.3 (OCH₃), 23.8 (*o*-CCH₃). The *ipso* C atom was not detected. IR (KBr, cm⁻¹): ν̄ 3119 w, 3048 s, 2993 m, 2969 m, 2899 m, 2856 m, 2785 s, 1579 m, 1561 w, 1459 m, 1446 s, 1376 m, 1275 m, 1267 m, 1201 s, 1154 m, 1114 m, 1020 vs, 947 w, 872 w, 792 m, 751 vs, 738 vs, 644 w, 616 s, 537 m, 490 w, 444 m, 430 s. MS (EI): 482 [(*o*-tolyl)₃Bi], 422 [M⁺], 391 [M⁺ − OCH₃], 300 [(*o*-tolyl)Bi], 182 [(CH₃)₂C₆H₄], 91 [(CH₃)₂C₆H₄].

[MeCp₂Mo(H)(Bi(*o*-tolyl)₂)]_∞, **4**, and [Cp₂Mo(H)(Bi(*o*-tolyl)₂)]_∞, **5**. Compound **3** (83.2 mg, 0.20 mmol) was dissolved in 5 mL of CH₂Cl₂, and a solution of 45.9 mg (0.18 mmol) of [MeCp₂MoH₂] in 2 mL of CH₂Cl₂ was added at room temperature. The resulting red solution was left to stir for 2 h, and subsequently, the solvent

- (2) (a) Roggan, S.; Limberg, C.; Ziemer, B. *Angew. Chem.* **2005**, *117*, 5393; *Angew. Chem., Int. Ed.* **2005**, *44*, 5259. (b) Roggan, S.; Limberg, C.; Brandt, M.; Ziemer, B. *J. Organomet. Chem.* **2005**, *690*, 5282.
 (3) Matano, Y.; Miyamatsu, T.; Suzuki, H. *Organometallics* **1996**, *15*, 1951.
 (4) Silavwe, N. D.; Castellani, M. P.; Tyler, D. R.; Beck, M. A.; Lichtenhan, J. D.; Doherty, N. M. *Inorg. Synth.* **1992**, *29*, 204.
 (5) Luo, L.; Lanza, G.; Fragala, I. L.; Stern, C. L.; Marks, T. J. *J. Am. Chem. Soc.* **1998**, *120*, 3111.

- (6) (a) Matano, Y.; Nomura, H.; Suzuki, H.; Shiro, M.; Nakano, H. *J. Am. Chem. Soc.* **2001**, *123*, 10954. (b) Breunig, H. J.; Ebert, K. H.; Schulz, R. E. *Z. Naturforsch.* **1995**, *50b*, 735.

was evaporated in vacuo to yield a red oil. Multiple extractions of the residue with small portions of hexane resulted in red colored hexane fractions and a white residue consisting of unreacted **3**. The unified hexane extracts were concentrated to approximately 2 mL and cooled to 4 °C. After a few days, red crystals had formed, which were collected and washed with hexane to yield 98 mg (0.15 mmol, 83%) of analytically pure **4**. Anal. Calcd for C₂₆H₂₉BiMo: C, 48.31; H, 4.52. Found: C, 48.51; H, 4.82. ¹H NMR (CD₂Cl₂): δ 7.59 (d, 2H, C₁₀H), 7.16 (m, 4H, C₁₀H), 6.88 (m, 2H, C₁₀H), 4.51 (bs, 2H, C_{Cp}H), 4.45 (bs, 2H, C_{Cp}H), 4.27 (bs, 2H, C_{Cp}H), 4.23 (bs, 2H, C_{Cp}H), 2.43 (s, 6H, C₁₀CH₃), 2.01 (s, 6H, C_{Cp}CH₃), -9.31 (s, 1H, MoH). ¹³C{¹H} NMR (CD₂Cl₂): δ 144.3 (C₁₀CH₃), 140.7/127.7/127.2/126.6 (C₁₀H), 97.3 (C_{Cp}CH₃), 84.0/83.1/80.8/79.6 (C_{Cp}H), 27.8 (C₁₀CH₃)/15.6 (C_{Cp}CH₃). IR (KBr, cm⁻¹): ν̄ 3101 w, 3084 w, 3047 m, 3024 sh, 2978 m, 2953 w, 2918 w, 2864 w, 1813 m, 1574 m, 1558 w, 1481 w, 1456 s, 1445 s, 1402 w, 1375 m, 1273 w, 1261 m, 1226 w, 1200 m, 1157 m, 1113 m, 1061 w, 1030 s, 1015 m, 978 w, 937 w, 926 w, 878 m, 841 m, 826 w, 787 s, 745 vs, 706 w, 600 w, 575 m, 432 s, 417 s.

The synthesis of **5** was performed analogously with 100 mg (0.24 mmol) of **3** and 54 mg (0.24 mmol) of [Cp₂MoH₂]. Yield: 120 mg (0.19 mmol, 79%). Anal. Calcd for C₂₄H₂₅BiMo: C, 46.62; H, 4.08. Found: C, 46.51; H, 4.40. ¹H NMR (CD₂Cl₂): δ 7.53 (d, 2H, C₁₀H), 7.15 (m, 4H, C₁₀H), 6.90 (m, 2H, C₁₀H), 4.57 (s, 10H, CpH), 2.42 (s, 6H, CCH₃), -9.40 (s, 1H, MoH). ¹³C{¹H} NMR (CD₂Cl₂): δ 144.2 (C_{Ar}CH₃), 140.3/127.8/127.4/126.7 (C_{Ar}H), 79.9 (C_{Cp}H), 27.7 (C_{Ar}CH₃). IR (KBr, cm⁻¹): ν̄ 3108 w, 3044 m, 3023 w, 2983 w, 2959 w, 2930 w, 2852 w, 1836 m, 1575 m, 1559 w, 1444 s, 1426 m, 1409 m, 1374 m, 1263 m, 1199 w, 1153 w, 1106 m, 1061 w, 1043 w, 1030 w, 1013 m, 993 m, 896 w, 864 w, 831 m, 820 m, 785 s, 751 vs, 741 vs, 587 m, 432 m, 417 m.

Deposition of Thick-Film Sensing Layer. According to a well-established protocol,⁷ the powder material was dispersed by mixing it in a mortar with an aqueous polyethylene imine (0.5 wt %) solution, and the resulting dispersion with a solid amount of 0.08 mol/L was then applied to an interdigital capacitor electrode structure. The substrate was first dried for 48 h at room temperature in air. After that it was held for 6 h at 700 °C in air to remove the organic residues.

Electrical Characterization. Electrical measurements were performed using a source meter at a measuring voltage of 1 V. The measurements were carried out in a temperature range between 500 and 400 °C in 25° steps (at lower temperature the resistance of the material exceeds the measurement limits). Reference measurements were performed in synthetic air, which was also used as the carrier gas for the test gases H₂, CO, NO₂, EtOH, and propylene, whereas for NO nitrogen was chosen as the carrier gas. For the gas-sensing experiments, the test gases were mixed with synthetic air to reach a continuous gas flow of 100 sccm each. Conditioning of the materials was carried out at 500 °C for 240 min in air and at the next temperatures for 90 min.

X-ray Data Collection. Suitable single crystals of **1** were obtained by slow evaporation of the solvent from a CH₂Cl₂ solution of the precipitate obtained by cooling the solution produced in the reaction between **II** and an equimolar amount of (*n*-C₄H₉)₄NOH (1 M solution in MeOH) in MeOH. Single crystals of **3** were obtained by cooling the filtrate of the reaction mixture leading to **3** to -30 °C. Suitable single crystals of **4** were obtained by cooling a hexane solution of **4** to 4 °C. The crystals were mounted on a glass fiber and then transferred to the cold nitrogen gas stream of

the diffractometer (Stoe IPDS I for **1** and **3**, Stoe IPDS2T for **4**) using Mo Kα radiation, λ = 0.71073 Å, and the structures were solved by direct methods (SHELXS-97),⁸ refined versus F² (SHELXL-97)⁹ with anisotropic temperature factors for all non-hydrogen atoms. The hydrogen atoms of the BiOH and MoH units in **1** and **4** were found from a difference Fourier map and freely refined in the following least-squares cycles. All remaining hydrogen atoms were added geometrically and refined using a riding model. The crystal of **3** was twinned with disordered tolyl groups at Bi.

For the structural characterization of the materials obtained from the polyol method, we carried out powder XRD measurements (Cu Kα, λ = 1.5418 Å) on thin films with a Huber Image Plate in transmission. The powder diffraction patterns were analysed using Stoe WinXPow 1.06 Software (Stoe & CIE GmbH).

Results and Discussion

Breaking Up II with Hydroxide. Previous studies probing the scope of breaking up polymer **II** by external donors to obtain more soluble molecular compounds had shown that treatment with Cp*MoO₃⁻ yields the complex anion **III** (Chart 1).^{2b} Envisaging the formation of novel compounds, possibly containing Mo—O—Bi—O—Bi units, via condensation reactions, we offered the most simple Lewis base, HO⁻, as a reagent in the form of NBu₄OH dissolved in MeOH. After the addition of NBu₄OH/MeOH, the stirring of the mixture, and the subsequent workup, colorless crystals were obtained that were investigated by means of X-ray analysis (Figure 1). It turned out that these crystals belonged to a [(*o*-tolyl)₂BiOH]_n coordination polymer, **1**, where the hydroxide ligands bridge two Bi centers each.

There is some very early work describing reactions (like treatment of Ph₂BiI with NaOH in EtOH and [(*p*-CH₃C₆H₄)₂-BiC]₂ with an alkaline Cu⁺ or Ag⁺ solution) whose products were assigned the formula Ar₂BiOH (Ar = Ph, *p*-tolyl) even though analytic/spectroscopic support is missing. In general, structurally characterized complexes containing an OH⁻ ligand covalently bonded to a Bi^{III} center are rather rare and include the hexanuclear cationic bismuth complex [Bi₆O₄(OH)₄](ClO₄)₆·7H₂O, **IV**, whose crystal structure was determined by X-ray diffraction, as well as by neutron diffraction studies,^{11a} and the related citrate cluster anion [Bi₆O₄(OH)(cit)₃(H₂O)₃]³⁻, **V**, where three of the hydroxide ligands in **IV** are substituted by the hydroxylic groups of three citrate ligands.^{11b} In clusters **IV** and **V**, the hydroxide anions act as μ₃ bridging ligands, while μ₂-OH bridges are found in the dinuclear compounds [(η²-NO₃)₂(tpy)Bi(μ-OH)₂Bi(tpy)(η²-NO₃)₂] (tpy = terpyridine), **VI**,¹² and [(η²-NO₃)₂(phen)Bi(μ-OH)₂Bi(phen)(η²-NO₃)₂] (phen = 1,10 phenanthroline), **VII**.¹³ A nonbridging terminal Bi—OH unit

(8) Sheldrick, G. M. *SHELXS-97, Program for Crystal Structure Solution*; University of Göttingen: Göttingen, Germany, 1997.

(9) Sheldrick, G. M. *SHELXL-97, Program for Crystal Structure Refinement*; University of Göttingen: Göttingen, Germany, 1997.

(10) (a) Rozenblumowna S.; Weil S. *Bull. Trav. Inst. Pharm. Etat* **1927**, *1*, 3. (b) Hartmann, H.; Habenicht, G.; Reiss, W. *Z. Anorg. Allg. Chem.* **1962**, *317*, 54.

(11) (a) Sundvall, B. *Inorg. Chem.* **1983**, *22*, 1906. (b) Asato, E.; Katsura, K.; Mikuriya, M.; Fujii, T.; Reedijk, J. *Chem. Lett.* **1992**, 1967.

(12) Junk, P. C.; Louis, L. M. *Z. Anorg. Allg. Chem.* **2000**, *626*, 556.

(7) Siemons, M.; Simon, U. *Sens. Actuators, B* **2006**, published online March 9, <http://dx.doi.org/10.1016/j.snb.2006.01.049>.

Table 1. Crystallographic Data of **1**, **3**, and **4**

	1	3	4
empirical formula	C ₁₄ H ₁₅ BiO	C ₁₅ H ₁₇ BiO	C ₂₆ H ₂₉ BiMo
fw	408.24	422.27	646.41
cryst size (mm)	0.40 × 0.36 × 0.28	0.30 × 0.22 × 0.18	0.20 × 0.17 × 0.16
cryst syst	orthorhombic	orthorhombic	triclinic
space group	<i>Pbca</i>	<i>Cm2a</i>	<i>P</i> $\bar{1}$
<i>a</i> (Å)	13.8069(7)	21.013(4)	7.9109(5)
<i>b</i> (Å)	8.4987(6)	16.391(3)	9.1244(7)
<i>c</i> (Å)	21.167(2)	4.1400(5)	15.7401(9)
α (deg)	90	90	79.837(5)
β (deg)	90	90	84.125(5)
γ (deg)	90	90	81.073(5)
<i>V</i> (Å ³)	2483.7(2)	1425.9(4)	1101.5(2)
ρ_{calcd} (g cm ⁻³)	2.183	1.967	1.949
<i>T</i> (K)	180(2)	180(2)	100(2)
abs corn	numerical		numerical
abs coeff (μ , mm ⁻¹)	14.173	12.347	8.555
<i>F</i> (000)	1520	792	620
index ranges	-18 ≤ <i>h</i> ≤ 18 -11 ≤ <i>k</i> ≤ 11 -28 ≤ <i>l</i> ≤ 28	-25 ≤ <i>h</i> ≤ 25 -20 ≤ <i>k</i> ≤ 20 -5 ≤ <i>l</i> ≤ 5	-10 ≤ <i>h</i> ≤ 11 -13 ≤ <i>k</i> ≤ 13 -23 ≤ <i>l</i> ≤ 23
θ range (deg)	3.41–29.37	3.15–25.96	3.57–31.84
reflns collected	3344	7439	24 860
independent reflns	3344 (<i>R</i> _{int} = 0.0000)	1418 (<i>R</i> _{int} = 0.0475)	7476 (<i>R</i> _{int} = 0.0395)
data/restraints/params	3344/1/151	1418/16/50	7476/0/262
GOF on <i>F</i> ² ^a	0.997	1.080	1.194
<i>Z</i>	8	4	2
<i>R</i> 1 ^b [<i>I</i> > 2 σ (<i>I</i>)]	0.0278	0.0215	0.0274
w <i>R</i> 2 ^c (all data)	0.0494	0.0532	0.0459
largest diff. peak and hole (e Å ⁻³)	1.706 and -1.962	1.188 and -0.692	1.560 and -1.782

^a GOF = $\{\sum[w(F_o^2 - F_c^2)^2]/(N_{\text{obsd}} - N_{\text{params}})\}^{1/2}$. ^b *R*1 = $\sum(|F_o| - |F_c|)/\sum|F_o|$. ^c w*R*2 = $[\sum(|F_o|^2 - |F_c|^2)^2/\sum(F_o^2)]^{1/2}$.

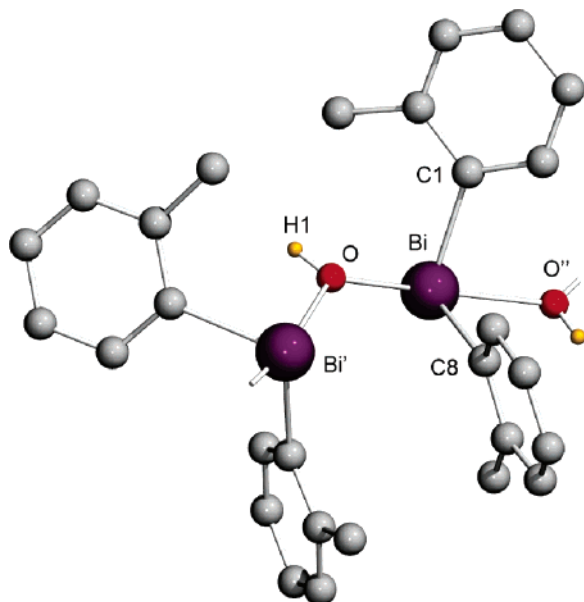


Figure 1. Molecular structure of **1**; all hydrogen atoms, except for the hydroxylic H atom, were omitted for clarity. Selected bond lengths (Å) and angles (deg): Bi–C1 = 2.255(4), Bi–C8 = 2.256(4), Bi–O = 2.319(3), Bi–O'' = 2.343(3), O–H1 = 0.83(4), Bi–O–Bi' = 135.6(2), O''–Bi–O = 161.09(3), C1–Bi–O = 87.0(2), C8–Bi–O = 82.0(2), C8–Bi–O'' = 81.9(2), C1–Bi–O'' = 85.4(2), C8–Bi–C1 = 97.7(2), Bi–O–H1 = 108(4).

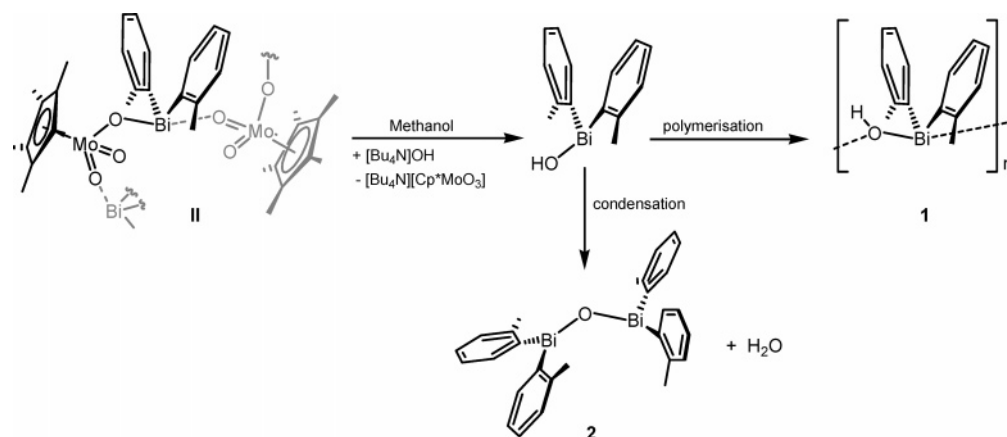
is only found in [Bi(dapt)(OH)] (H₂dapt = 2,6-diacetylpyridine bis (2-theonylhydrazone)), **VIII**.¹⁴

Compound **1** crystallizes as a coordination polymer where (*o*-tolyl)₂BiOH moieties are linked via intermolecular interactions between the hydroxide ligands and the bismuth atoms of adjacent molecules. The bismuth center is coordinated in

a pseudo-trigonal bipyramidal fashion (also called “seesaw”) where the oxygen atoms occupy the apical positions. The angle between them amounts to 161.09(3)° indicating a distorted coordination. Aggregation of R₂BiX molecules (where X represents an electronegative substituent) under the formation of polymeric chains is not uncommon and reflects the lewis acidic character of the Bi^{III} center.¹⁵ The linkages between the monomeric units are accomplished via secondary interactions between lone pairs of the X ligand and σ^* Bi–X acceptor orbitals of neighboring molecules, which results in the observed trans arrangement of the electronegative ligands in the polymers formed. Similar structural features are observed, for example, in **II**,^{2a} where the O–Bi–O angle is 170.46(9)°, or in a series of bismuth halides ligated by organometallic complex fragments such as, for example, [BiX{Mo(CO)₃Cp}₂] (X = Cl or Br) with a Cl–Bi–Cl angle of 151.6(1)° and a Br–Bi–Br angle of 148.2(1)°.¹⁶ Deviation of the X–Bi–X units from linearity indicates a less-efficient overlap between X and the σ^* Bi–X orbitals and thus a weakening of the secondary bond; in fact, the BiX₂ angle correlates with the strength of this interaction. Moreover, with the increasing strength of the secondary bond, the corresponding primary bond is weakened so that

- (13) Barbour, L. J.; Belfield, S. J.; Junk, P. C.; Smith, M. K. *Aust. J. Chem.* **1998**, *51*, 337.
 (14) Battaglia, L. P.; Bonamartini Corradi, A.; Pelizzi, C.; Pelosi, G.; Tarasconi, P. *J. Chem. Soc., Dalton Trans.* **1990**, 3857.
 (15) Roggan, S.; Limberg, C. *Inorg. Chim. Acta* in press.
 (16) (a) Clegg, W.; Compton, N. A.; Errington, R. J.; Norman, N. C.; Tucker, A. J.; Winter, M. J. *J. Chem. Soc., Dalton Trans.* **1988**, 2941.
 (b) Clegg, W.; Compton, N. A.; Errington, R. J.; Fisher, G. A.; Hockless, D. C. R.; Norman, N. C.; Williams, N. A. L.; Stratford, S. E.; Nichols, S. J.; Jarrett, P. S.; Orpen, A. G. *J. Chem. Soc., Dalton Trans.* **1992**, 193.

Scheme 1

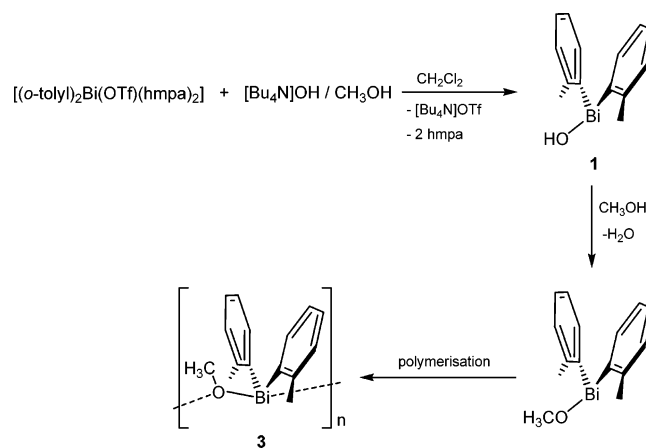


in extreme cases the two Bi–X bond lengths align. In **1**, the first Bi–O bond length is 2.319(3) Å being only a little shorter than the second Bi–O' bond (2.343(3) Å), so that a distinction between the covalently bonded O atom and the coordinatively bonded O atom (i.e., primary vs secondary interaction) is hardly possible. These similar Bi–O bond lengths, as well as the nearly linear O–Bi–O unit, suggest a strong secondary bond. In the case of **II**, where the O–Bi–O angle is even closer to 180° (170.46(9)°), the Bi–O bond distances are nearly identical, too (2.310(2) vs 2.385(2) Å). The Bi–OH bond lengths of dinuclear complexes **VI** and **VII** are similar (2.20(1) and 2.32(1) Å in the terpyridine derivative, **VI**, and 2.214(3) and 2.232(3) Å in the more symmetrically bridged **VII**). As a result of the planar Bi₂O₂ diamond core structure, the O–Bi–O angles are very acute and amount to 66.5(4)°. Consequently, the acceptor orbital for the linking of one (formally separated) Bi–OH unit to the second Bi center cannot be the Bi–OH σ* orbital of the latter, and hence, no bond elongation as observed in **1** occurs resulting in shorter Bi–OH bonds in **VI** and **VII**, as compared to those in **1**. For the abovementioned complexes, the shortest Bi–OH bond length is found in **VIII** (2.08(1) Å) which contains an isolated Bi–OH bond without any bridging interaction.

Accordingly, the addition of hydroxide to **II** breaks up all of the Mo–O–Bi contacts to give a homometallic compound **1**; the condensation product [(*o*-tolyl)₂Bi–O–Bi(*o*-tolyl)₂], **2**, (that has been mentioned previously^{6a} as a reaction byproduct according to ¹H NMR spectroscopic assignments) and [NBu₄][Cp*MoO₃]¹⁷ were identified as additional products by means of NMR spectroscopy (Scheme 1), and unfortunately, these crystallize together with **1** which consequently can only be separated from them in small amounts mechanically.

Compound **1** is by far the most simple well-characterized Bi–OH complex known so far, so that it seemed to be an interesting compound in its own right (for instance as a starting material for further syntheses). Hence, attempts were made to prepare it in a higher yield via the reaction of [(*o*-tolyl)₂Bi(hmpa)₂]SO₃CF₃³ with NBu₄OH in MeOH. These might have been successful in the first place, but then

Scheme 2



replacement of hydroxide by methoxide ligands occurred so that [(*o*-tolyl)₂BiOMe]_n, **3**, was isolated instead of **1** (Scheme 2). The result of an X-ray crystal structure determination is shown in Figure 2.

In recent years, the increasing interest in oxidic materials based on bismuth has led to the synthesis of numerous soluble bismuth alkoxides which were employed as starting materials for sol gel or chemical vapor-deposition processes. However, most of the structurally characterized bismuth(III) alkoxides are homoleptic: for example, [Bi(OC₆H₃Me₂-2,6)₃],¹⁸ [Bi(OCH(CF₃)₂)₃(thf)₂],¹⁹ **IX**, [Bi(OCH₂CH₂-OCH₃)₃]_∞,²⁰ **X**, and [Bi(OEt)₃]₈,^{20c,21} **XI**. M. Wieber and U. Baudis in 1978 reported the first nonhomoleptic Bi^{III}-alkoxide complexes with the general formula Ph₂BiOR (R = Me, Et, *i*Pr, Ph), as well as CH₃Bi(OR)₂ (R = Me, Et, *i*Pr), which were prepared by metathetical reactions between the organobismuthbromides and the corresponding sodium

(18) Evans, W. J.; Hain, J. H., Jr.; Ziller, J. W. *J. Chem. Soc., Chem. Commun.* **1989**, 1628.

(19) (a) Jones, C. M.; Burkart, M. D.; Whitmire, K. H. *Angew. Chem.* **1992**, *104*, 466; *Angew. Chem., Int. Ed. Engl.* **1992**, *31*, 451. (b) Jones, C. M.; Burkart, M. D.; Bachman, R. E.; Serra, D. L.; Hwu, S.-J.; Whitmire, K. H. *Inorg. Chem.* **1993**, *32*, 5136.

(20) (a) Matchett, M. A.; Chiang, M. Y.; Buhro, W. E. *Inorg. Chem.* **1990**, *29*, 358. (b) Massiani, M.-C.; Papiernik, R.; Hubert-Pfalzgraf, L. G.; Daran, J.-C. *J. Chem. Soc., Chem. Commun.* **1990**, 301. (c) Massiani, M.-C.; Papiernik, R.; Hubert-Pfalzgraf, L. G.; Daran, J.-C. *Polyhedron* **1991**, *10*, 437.

(21) (a) Kessler, V. G.; Turova, N. Ya.; Turevskaya, E. P. *Inorg. Chem. Commun.* **2002**, *5*, 549.

(17) Sundermeyer, J.; Radius, U.; Burschka, C. *Chem. Ber.* **1992**, *125*, 2379.

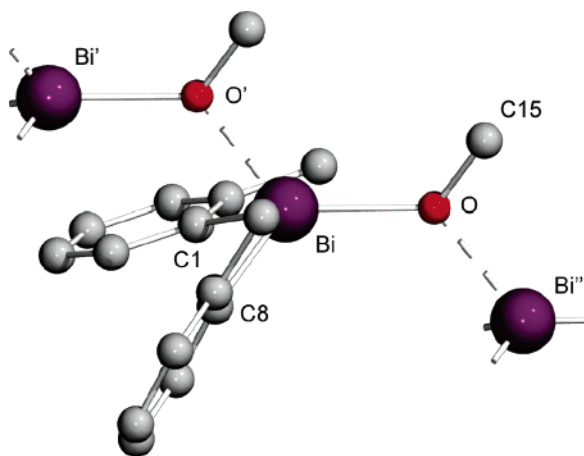


Figure 2. Molecular structure of **3**; all hydrogen atoms were omitted for clarity. Selected bond lengths (Å) and angles (deg): Bi–C1 = 2.270(6), Bi–C8 = 2.308(6), Bi–O = 2.295(5), Bi–O' = 2.399(5), O–C15 = 1.42(2), Bi–O–Bi'' = 123.7(3), O'–Bi–O = 123.7(3), C1–Bi–O = 129.4(2), C8–Bi–O = 117.5(2), C1–Bi–O' = 90.9(2), C8–Bi–O' = 89.2(2), C1–Bi–C8 = 96.2(3), Bi–O–C15 = 124.5(5), C15–O–Bi'' = 111.7(5).

alkoxides. However, none of them could be characterized via X-ray diffraction, and their preparations involve tedious filtrations of the alkali salt byproducts.²² In this context it should also be noted that [(*o*-tolyl)₂BiOMe] has been mentioned before as a byproduct of the reaction of [(*o*-tolyl)₃Bi=N–C(O)–Ar] with methanol in an NMR tube experiment: the signals in the ¹H NMR spectrum of the crude product were “tentatively assigned to [(*o*-tolyl)₂BiOMe] but attempts to prepare the sample independently failed”.⁶ In fact the only structurally characterized diorganobismuthalkoxide complexes we are aware of are the *aryloxides* 10-arylphenothiabismine 5,5-dioxide (aryl = 2-methoxyphenoxy and 4-methoxyphenoxy)²³ and [Et₂Bi(OAr)]_∞,²⁴ (Ar = C₆F₅ (**XII**), Ph (**XIII**)). Compound **3** represents a diorgano bismuth alkoxide, and its bismuth center is covalently bound to two carbon atoms of the tolyl ligands and an oxygen atom of the methoxy ligand. As in **1**, an additional secondary interaction with the methoxy oxygen of a neighboring molecule is observed leading to a one-dimensional polymeric structure. However, in contrast to **1** the O'–Bi–O angle is only 123.7(3)°, indicating that this secondary interaction is comparatively weak. The structure can thus not be described as ψ -trigonal bipyramidal, and the assignment to a ψ -square pyramidal geometry which could have been expected if the lone pair was stereoactive does not seem to be appropriate, either. The structure should thus be discussed most adequately as being distorted tetrahedral. Variations between these two different structural types have been observed previously for 10-electron AB₄E compounds, and electronic reasons (e.g., π -donor properties of ligands) were discussed.²⁵ However, **3** differs from **1** only in that a proton has been exchanged by a methyl group, and therefore, the reason for

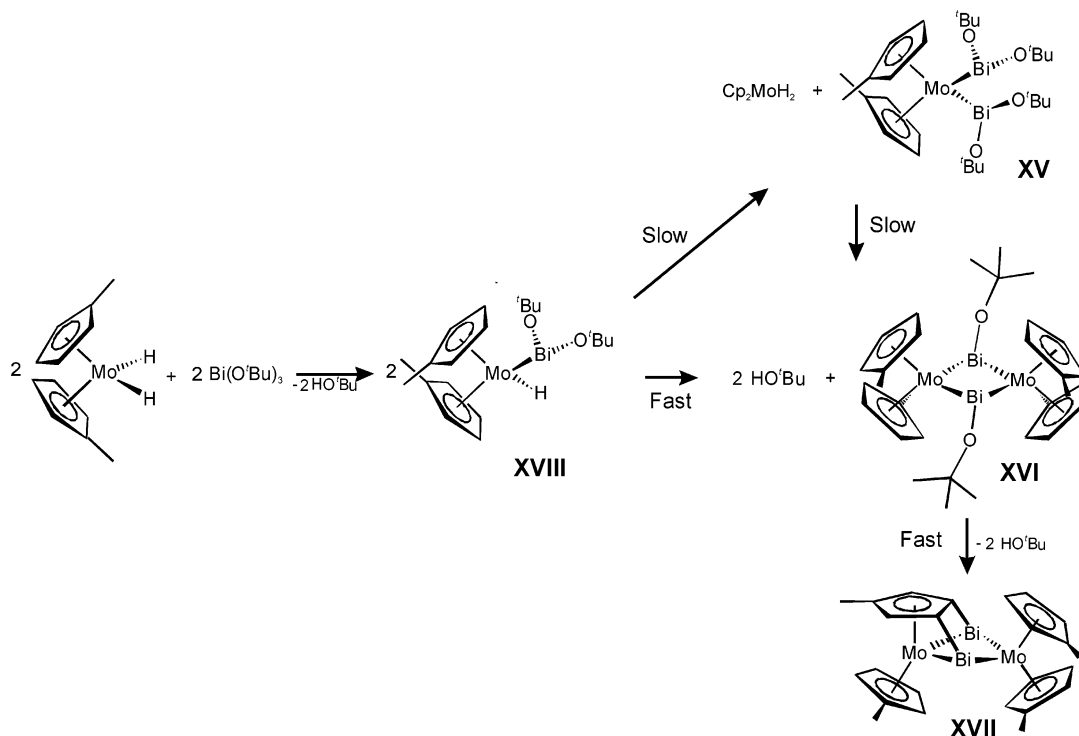
its peculiar structural behavior remains unclear, particularly considering the structures of the aryloxides **XII** and **XIII**, which consist of polymeric chains similar to the ones of **1** and **3** but contain Bi centers in a seesaw-like coordination sphere, as found in hydroxide **1**. The Bi–O bonds in **3** (2.295(5) and 2.399(5) Å) are more distinct than those in **1** or in **II**, which again points to a weak secondary interaction. They are shorter than those in aryloxides **XII** (2.4105(7) and **XIII** (2.382(7) Å), where the secondary bonds are as strong as the primary ones leading to equal distances. Because a comparison with other diorganobismuthalkoxides (where the alkoxide ligand is aliphatic) is not possible (vide supra), the structural parameters of **3** involving the alkoxidic units are compared with the ones of homoleptic bismuth alkoxides bearing aliphatic alkoxide ligands. Because of the strong Lewis acidity of the Bi^{III} center, there is only one monomeric Bi(OR)₃ complex known with R representing a saturated hydrocarbon residue, Bi(OCPh₃)₃, whose Bi–O bonds average 2.074(4) Å which is typical for terminal Bi–alkoxide ligands.^{26a} In other cases with less bulky organic residues, dimers or oligomers are formed that exhibit terminal OR ligands with or without a trans-coordinated OR counterligand. Not surprisingly, the Bi–O bonds displayed by OR ligands positioned trans to a vacant coordination site compare to those in Bi(OCPh₃)₃ and are shorter than those in **3** (e.g., 2.064(8), 2.07(2), and 2.06 (averaged) Å in **IX**, **X**, and **XI**, respectively). On the other hand, as expected, the Bi–O bond lengths found in trans RO–Bi–OR arrangements compare to those in **3**: the Bi–O distances are 2.188(7) Å in **IX**, 2.20(1) Å in **X** or 2.265(8) and 2.285(9) Å in the potassium-(*tert*butoxy) bismuthate K[(*Ot*Bu)₄Bi], **XIV**.^{26b}

The question of why the synthesis shown in Scheme 1 proceeds to give **1** and not **3** cannot be answered with certainty. Compound **1** is poorly soluble in methanol, which was used for the reaction shown in Scheme 1, so that rapid precipitation may have prevented it from undergoing alcoholysis with MeOH, while some condensation to **2** could still proceed. This hypothesis is supported by the slow conversion of **1** to **3** and **2** (accompanied by some decomposition to (*o*-tol)₃Bi) that can be observed when pure **1** (vide infra) is stirred in dry MeOH for a prolonged time. The addition of CH₂Cl₂ to a suspension of **1** in MeOH accelerates the formation of **3** and, at the same time, reduces that of **2**. If this reactivity of pure **1** is considered, the formation of **3**, as shown in Scheme 2, can be well understood in terms of the solubilities/aggregation and precipitation rates in different solvents. In solution, the initially formed hydroxide reacts readily with any MeOH present, while the condensation to **2** still occurs. The latter can be suppressed by the addition of excess MeOH (Experimental Section). This alcoholysis generates water, and it seems peculiar that **3** should be resistant to that. However, during the reaction, small amounts

(22) (a) Wieber, M.; Baudis, U. *Z. Anorg. Allg. Chem.* **1978**, *439*, 134. (b) Wieber, M.; Baudis, U. *Z. Anorg. Allg. Chem.* **1978**, *439*, 139.
 (23) Murafuji, T.; Nagasue, M.; Tashiro, Y.; Sugihara, Y. *Organometallics* **2000**, *19*, 1003.
 (24) Whitmire, K. H.; Hutchison, J. C.; McKnight, A. L.; Jones, C. M. *J. Chem. Soc., Chem. Commun.* **1992**, 1021.

(25) (a) Gimarc, B. M.; Khan, S. A. *J. Am. Chem. Soc.* **1978**, *100*, 2340. (b) Clegg, W.; Compton, N. A.; Errington, R. J.; Fisher, G. A.; Hockless, D. C. R.; Norman, N. C.; Orpen, A. G.; Stratford, S. E. *J. Chem. Soc., Dalton Trans.* **1992**, 3515.
 (26) (a) Hanna, T. A.; Keitany, G.; Ibarra, C.; Sommer, R. D.; Rheingold, A. L. *Polyhedron*, **2001**, *20*, 2451. (b) Veith, M.; Yu, E.-C.; Huch, V. *Chem.–Eur. J.* **1995**, *1*, 26.

Scheme 3



of a white precipitate form, which is purely inorganic in nature according to spectroscopic analysis. A possible explanation is, therefore, that all water generated is scavenged in the course of successive reactions that lead to the *complete* decomposition of a small part of **3**.

As outlined above diorganobismuthalkoxides are more prominent than bismuthhydroxides; however, well-characterized examples that are available in high yields are rare. Therefore, **3** might be an interesting starting material for future research, too, and the experiments described below support this potential.

Turning the attention back onto **1** first and a suitable synthesis leading to it in a pure form, we decided to reinvestigate the reaction between $[(o\text{-tolyl})_2\text{Bi}(\text{hmpa})_2]\text{SO}_3\text{-CF}_3$ ³ and NBu_4OH in a mixture of *thf*/water as the solvent. This indeed led to a white precipitate consisting of **1** as shown by elemental analysis and IR spectroscopy. Dissolution of this solid in CDCl_3 or C_6D_6 for NMR spectroscopic investigations, however, only showed signals for $(o\text{-tolyl})_2\text{Bi-O-Bi}(o\text{-tolyl})_2$, **2**, and H_2O , in addition to signals belonging to small quantities of a second unidentified component (i.e., dissolution in nonprotic solvents immediately triggers the condensation process (also compare, for instance, ref 6b)). The latter can also be performed on a preparative scale, thus offering a synthetic route to **2** which so far had only been characterized via a ^1H NMR spectrum:^{6a} recrystallization of the abovementioned white precipitate **1** from hot toluene leads to a different white precipitate which was shown by analysis to be pure **2**. Accordingly, all results can be summarized as follows: Reactions of **II** or $[(o\text{-tolyl})_2\text{Bi}(\text{hmpa})_2]\text{SO}_3\text{CF}_3$ with NBu_4OH lead to **1** initially. However, appreciable amounts of **1** can only be isolated when precipitation occurs rapidly, as in the presence of alcohols

and water (in many instances, we noted that even small amounts of water are very beneficial). Otherwise, it is labile in solution with respect to condensation reactions leading to **2**; it can only escape them if precipitation proceeds faster than condensation. In the presence of MeOH , the alcoholysis of **1** to **3** is apparently faster than its condensation to **2**, so that **3** is isolated predominantly.

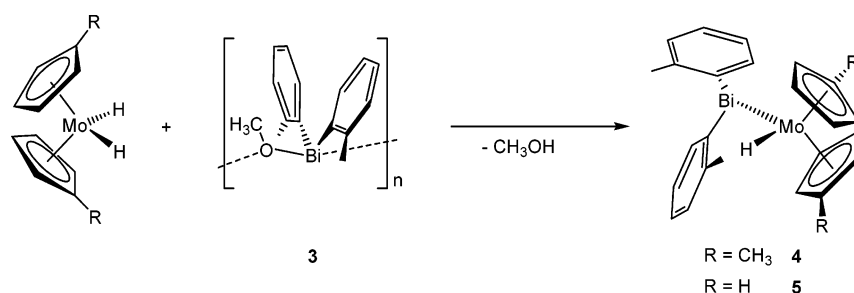
Breaking Up II with Molybdocenedihydrides. It further seemed interesting to explore the behavior of **II** in contact with molybdocenedihydrides: Previously, it had been shown that $[\text{M}^{\text{c}}\text{Cp}_2\text{MoH}_2]$ and $[\text{Bi}(\text{O}t\text{Bu})_3]$ react to give, in course of the reactions shown in Scheme 3, three novel complexes (**XV**, **XVI**, and **XVII**) which were isolated and characterized.²⁷

C-H-activation reactions initiated by complex-induced proximity effects in **XVI** allow for the formation of **XVII** featuring a, until then, unprecedented bonding situation, where a planar $\mu_3\text{-}\eta^5\text{:}\eta^1\text{:}\eta^1\text{-MeCp}$ ligand bridges three metal centers that are additionally linked via metal bonds. As a reaction intermediate, the novel molybdocene monohydride species **XVIII** was identified by NMR spectroscopy, but it eluded isolation as its half-life in solution is only ~ 15 min. If the low Brønsted acidity of molybdocene dihydride is taken into account, its reaction with the bismuthalkoxide to form **XVIII** under elimination of alcohol should not proceed by a simple acid-base reaction but via a precursor complex involving the lone pair of either the molybdocene unit or the bismuth center.^{28a} Hence, the question of whether

(27) Roggan, S.; Limberg, C.; Ziemer, B.; Brandt, M. *Angew. Chem.* **2004**, *116*, 2906; *Angew. Chem., Int. Ed.* **2004**, *43*, 2846.

(28) (a) Hunger, M.; Limberg, C.; Kaifer, E.; Rutsch, P. *J. Organomet. Chem.* **2002**, *641*, 9. (b) Roggan, S.; Schnakenburg, G.; Limberg, C.; Sandhöfner, S.; Pritzkow, H.; Ziemer, B. *Chem.—Eur. J.* **2005**, *11*, 225.

Scheme 4



molybdocene dihydride is also capable of breaking up the polymer **II**, either by formation Mo–OH/Bi–Mo units or by generation Bi–OH/Mo–Mo moieties, arose. The reaction of [^{Me}Cp₂MoH₂] (or [Cp₂MoH₂]) with **II** in benzene led to a red solution that according to ¹H NMR spectroscopic results contained the known^{17,29} [Cp*₂Mo₂O₅] as well as a new product whose data in combination with those obtained for **XVIII** hinted to the formation of a monohydride compound [^RCp₂Mo(H)(Bi(*o*-tolyl)₂)], (R = Me (**4**), H (**5**)); remarkably, in contrast to **XVIII**, compounds **4** and **5** appeared to be thermally stable. Because they could not be isolated from this mixture in a pure form, we attempted an alternative synthesis, which we hoped would provide a purer product on a larger scale, starting from the molybdocene dihydrides and **3**, by analogy to the formation of **XVIII** according to Scheme 3 (see Scheme 4).

Indeed, **4** and **5** formed in good yields which also allowed crystallization. The result of the single-crystal X-ray analysis for **4** is shown in Figure 3.

As mentioned above, in our studies concerning the [^{Me}Cp₂MoH₂]/[Bi(*o*TBu)₃] system, there was ¹H NMR spectroscopic evidence that the reaction mixture leading to **XVI** contained [^{Me}Cp₂Mo(H)(Bi(*o*TBu)₂)], **XVIII**, intermediately, and **4** clearly represents a stable derivative of it. In **4**, the common structure of M(IV) Cp₂ML₂ complexes is retrieved with a bent-sandwich configuration of the cyclopentadienyl ligands about the metal. The bending angle in **4** is 145.3°; thus it

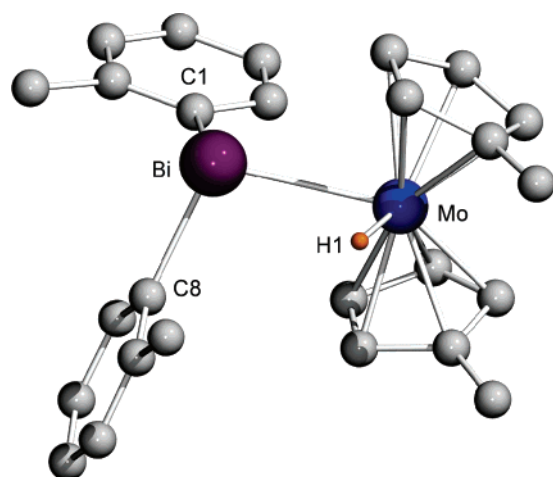


Figure 3. Molecular structure of **4**; all hydrogen atoms, except for those of the hydride ligand, were omitted for clarity. Selected bond lengths (Å) and angles (deg): Mo–Bi = 2.8976(3), Mo–H1 = 1.56(5), Bi–C1 = 2.279(3), Bi–C8 = 2.292(3), H1–Mo–Bi = 72(2), C1–Bi–C8 = 94.8(2), C1–Bi–Mo = 103.14(6), C8–Bi–Mo = 102.03(7).

compares well with the value of 145.8° in [Cp₂MoH₂]^{30a} or 143.3° in **XV**,²⁷ but is slightly smaller than the one in [^{Me}Cp₂MoH₂] (149.5(1)°).^{30b} The Mo–Bi bond length amounts to 2.8976(3) Å and is thus similar to those found in the other compounds with bismuth atoms bonded to the Cp₂Mo or ^{Me}Cp₂Mo moieties. These range from 2.788(2) Å in [Cp₂Mo{Bi(OCH(CF₃)₂)₂}₂]^{28a} to 2.966(2) Å in the tetranuclear compound [{Cp₂Mo}₂{μ-Bi(*o*TBu)₂}₂]^{28b} which has a structure similar to that of **XVI**. The Mo–H bond length of 1.56(5) Å is significantly shorter than that in [Cp₂MoH₂] (neutron diffraction, 1.685(3) Å)^{30a} or [^{Me}Cp₂MoH₂] (1.63(3) Å).^{30b} The only known homologous molybdocenemonohydrides that have so far been structurally characterized appear to be [Cp₂Mo(H)(μ-PPh₂)Mn(CO)₂Cp]³¹ and the ionic complex [Cp₂Mo(H)(PPh₃)]₂I⁺,³² while no compounds containing one As or Sb atom bonded to the Mo center are known. In both cases, the Mo–H bond is longer than in **4** (1.71(9) and 1.74(8) Å, respectively). Mo–H bond distances more similar to the one in **4** are found in the complexes [Cp₂Mo(H)(SiH₂(C₅Me₄H))]³³ **XIX** (1.58(6) Å), and [Cp₂Mo(H)(SnMe₃)]³⁴ **XX** (1.60(5) and 1.51(6) Å in two independent molecules in the unit cell).

The H–Mo–Bi angle in **4** is 72.0(3)° and, as expected, is somewhat smaller than the Bi–Mo–Bi angles (74.76(3)–77.41(3)°) which were found in the above-mentioned [MoBi₂] complexes (replacement of BiR₂ by H). The angle is similar to the H–Mo–E angles measured for the related group 14 compounds mentioned (e.g., 76(2)° in **XIX** (E = Si) or 67.5 and 69.5° in **XX** (E = Sn)). The aryl ligands surround the Bi center in a manner similar to that of the *o*TBu ligands coordinated to the Bi atom in **XV** (i.e., they show an acute C–Bi–C angle of 94.8(2)°, indicating the predominant p character of the orbitals involved).

Accordingly, it can be confirmed that **4** and **5** are products of the reaction between molybdocenedihydrides and **II**, and

- (29) (a) Herberhold, M.; Kremnitz, W.; Razavi, A.; Thewalt, U. *Angew. Chem.* **1985**, *97*, 603; *Angew. Chem., Int. Ed. Engl.* **1985**, *24*, 601. (b) Saurenz, D.; Demirhan, F.; Richard, P.; Poli, R.; Sitzmann, H. *Eur. J. Inorg. Chem.* **2002**, 1415.
- (30) (a) Schultz, A. J.; Stearley, K. L.; Williams, J. M.; Mink, R.; Stucky, G. D. *Inorg. Chem.* **1977**, *16*, 3303. (b) Stender, M.; Oesen, H.; Blaurock, S.; Hey-Hawkins, E. *Z. Anorg. Allg. Chem.* **2001**, *627*, 980.
- (31) Barre, C.; Kubicki, M. M.; Leblanc, J.-C.; Moise, C. *Inorg. Chem.* **1990**, *29*, 5244.
- (32) Azevedo, C. G.; Calhorda, M. J.; Carrondo, M. A. A. F. de C. T.; Dias, A. R.; Félix, V.; Romao, C. C. *J. Organomet. Chem.* **1990**, *391*, 345.
- (33) Petri, S. H. A.; Neumann, B.; Stammer, H.-G.; Jutzi, P. *J. Organomet. Chem.* **1998**, *553*, 317.
- (34) Protsky, A. N.; Bulychev, B. M.; Soloveichik, G. L.; Belsky, V. K. *Inorg. Chim. Acta* **1986**, *115*, 121.

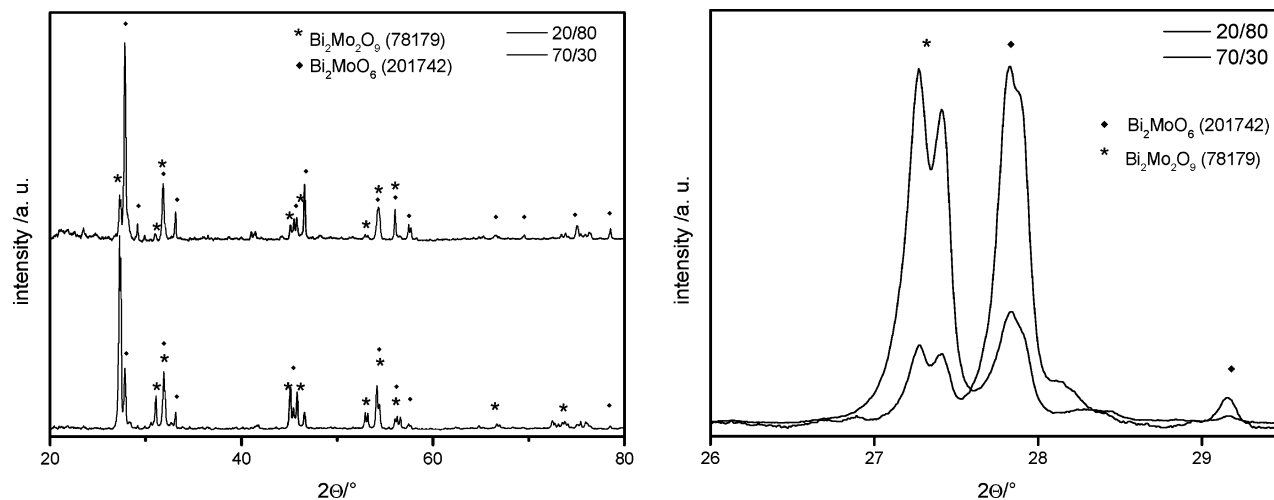


Figure 4. X-ray diffraction patterns of material A and B from complex II.

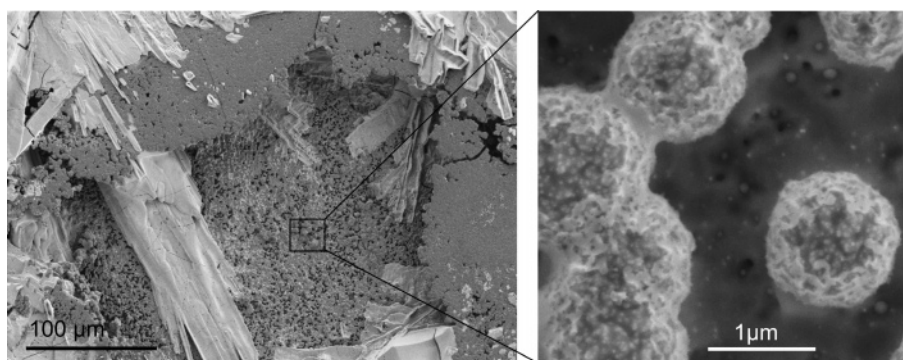


Figure 5. SEM pictures of material A.

this, as well as the identification of $[\text{Cp}_2^*\text{Mo}_2\text{O}_5]$ as the byproduct, suggests an attack of a Mo–H function at the Bi–O–Mo bonds under the formation of Mo–Bi and Mo–OH linkages; the Mo–OH units then undergo intermolecular condensation processes to yield the Mo–O–Mo moiety in $[\text{Cp}_2^*\text{Mo}_2\text{O}_5]$. The stabilities of **4** and **5** are remarkable considering that they differ from **XVIII** only in the residues at the bismuth centers.

Hence, the first representative of the hitherto elusive substances $[\text{Cp}_2\text{Mo}(\text{H})(\text{BiR}_2)]$ has been obtained simply by variation of R from the *tert*-butoxy ligands to the *o*-tolyl ligands, and **3** has been very helpful as a starting material for a high-yield synthesis.

Precursor Chemistry with II and Other Mo/Bi Compounds. Finally, we were interested in whether **II** could serve as a starting material in the polyol method^{35–37} to produce bismuthmolybdate ($\text{Bi}_2\text{O}_3 \cdot n\text{MoO}_3$, $n = 1, 2, \text{ or } 3$) nanoparticles that might find application in gas sensing, catalysis, etc. Hence, 160 mg of complex **II** was dispersed in 10 mL of diethylene glycol (DEG) and heated to 120 °C under vigorous stirring until a clear solution was obtained. Subsequently, 0.4 mL of deionized water in route A and 0.4

mL 65% nitric acid in route B were added as hydrolyzing agents, respectively. The emerging suspensions were heated for 5 h to 170 °C, and then they were allowed to cool to room temperature. To obtain crystalline materials, the suspensions were dried at 400 °C (1 h), and the solid obtained was then annealed at 700 °C for 12 h. A detailed description of this synthesis method can be found in ref 37. The initial characterization of the products was carried out by powder XRD measurements on thin films, and Figure 4 shows the X-ray diffraction patterns for the products obtained from routes A and B.

It becomes evident that in both cases a mixture of $\text{Bi}_2\text{Mo}_2\text{O}_9$ and Bi_2MoO_6 was formed. For route A, about 70% Bi_2MoO_6 was achieved, and for route B, we obtained about 80% $\text{Bi}_2\text{Mo}_2\text{O}_9$. No further byproduct was identified. SEM characterization of the materials showed that not only nanoparticles were formed. Figures 5 and 6 show the SEM pictures of the products obtained from routes A and B, respectively.

In both cases, mixtures of needles (crystallites) and nanoparticles are found. The sizes of the primary particles are around 30–60 nm (route A) and 80–200 nm (route B), whereas the needles span from the micrometer to millimeter range. From the energy-dispersive X-ray microanalysis (EDX) measurements, an accurate assignment to the different products could not be made. Considering the potential of **II** to act as a single-source precursor for the bismuthmolybdate

(35) Figlarz, M.; Fievet, F.; Lagier, J. P. EU 0113281, US A 4539041, JP 04024402, 1982.

(36) Feldmann, C.; Jungk, H.-O. *Angew. Chem.* **2001**, *113*, 372; *Angew. Chem., Int. Ed.* **2001**, *40*, 359.

(37) Siemons, M.; Weirich, Th.; Mayer, J.; Simon, U. *Z. Anorg. Allg. Chem.* **2004**, *630*, 2083.

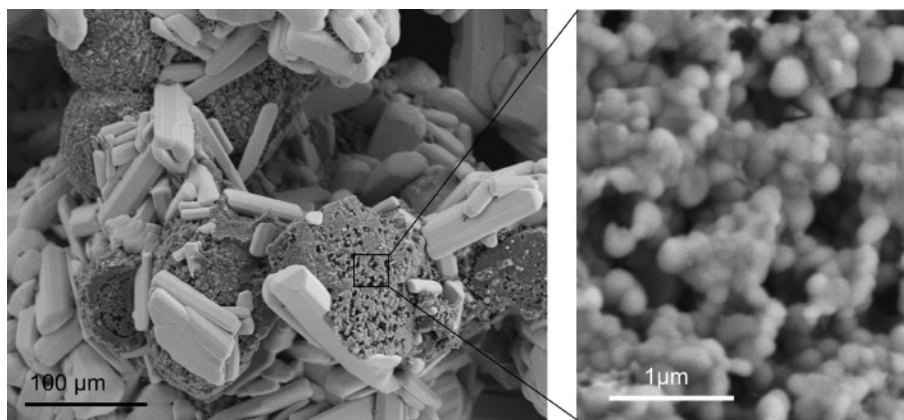


Figure 6. SEM pictures of material B.



Figure 7. Homogeneous sensor layer formed from material A (Bi_2MoO_6 (70%)/ $\text{Bi}_2\text{Mo}_2\text{O}_9$ (30%)).

materials, we thus concluded that it facilitates mixing on the molecular level and the avoidance of sample inhomogeneities; however, the preparation of pure phases seems to not be possible because the crystallization of more than one phase occurs at the calcination temperature. In addition, the chelating effect of the diethylene glycol used as the solvent seems to not be strong enough for the exclusive preparation of nanoparticles. On the other hand, the product distribution can be influenced by the use of different hydrolysis agents.

However, for various applications (e.g., as catalyst for the oxidation of light olefins³⁸ and gas-sensing materials for hydrocarbons),³⁹ bismuthmolybdates are employed not only in form of single-phases but also as mixtures of different bismuth molybdate materials.

Therefore the product obtained via preparation A was used for further investigations with respect to gas-sensing properties. A photograph of the sensing layer on the interdigital capacitor structure is shown in Figure 7. The sensing layer was around 4 mm in diameter. The distance between electrodes was around 110 μm .

The test gas sequence was H_2 (25 ppm), air, CO (50 ppm), air, NO (5 ppm), air, NO_2 (5 ppm), air, EtOH (40 ppm), air, propylene (25 ppm), air. The intermediate measurements in air were intended to verify the recovery of the resistance, before the next test gas was applied. The relative humidity

of the gases was 45% at room temperature so that the measurements were performed in a typical humidity range representative for ambient conditions. For sample conditioning, a preliminary gas flow was applied over 30 min to reach equilibrium. A detailed description of the experimental setup can be found in ref 40.

A plot of conductance versus temperature for the compounds prepared is shown in Figure 8, which indicates that the conductivity is thermally activated, as expected. According to the Arrhenius relation, an activation energy, E_A , of the process could be estimated to be 0.98 eV. Figure 9 shows the sensitivity dependence versus the temperature. The absolute sensitivity, S , of a material to a test gas is defined by

$$S = \frac{R_g}{R_r} - 1 \quad R_g > R_r$$

$$S = \frac{R_r}{R_g} - 1 \quad R_g < R_r$$

where R_g is the resistance obtained under test gas and R_r is the reference resistance value for a measurement under synthetic air.

Only NO, propylene, and ethanol are shown because no sensitivity was observed toward the other gases. Over the temperature range investigated, a pronounced sensitivity toward ethanol could be found, while the sensitivities toward nitrogen oxide and propylene were only weak.

To measure the response time of the sample, conductivity measurements at a single frequency (100 Hz) with an impedance analyzer were performed. The 100 Hz frequency was chosen to remain in the quasi-dc plateau (i.e., the frequency-independent part at low frequencies of the impedance spectra). While each measurement took 1.5 s, the time interval between the measurements was 4 s.

Figure 10 shows the response and recovery time, τ_{50} (i.e., time needed to reach 50% of the maximum response upon exposure to ethanol), at 500 °C. The material responds fast upon exposure to 40 and 60 ppm of ethanol ($\tau_{50} < 15$ s), and the recovery time is slightly higher ($\tau_{50} \approx 18$ s). An

(38) Le, M. T.; Van Well, W. J. M.; Stoltze, P.; Van Driessche, I.; Hoste, S. *Appl. Catal., A* **2005**, *282*, 189.

(39) Morrison, S. R.; Hykaway, N. J.; Sears, W. M.; Frindt, R. F. US 5082789, 1992.

(40) Simon, U.; Sanders, D.; Jockel, J.; Brinz, T. *J. Comb. Chem.* **2005**, *7*, 682.

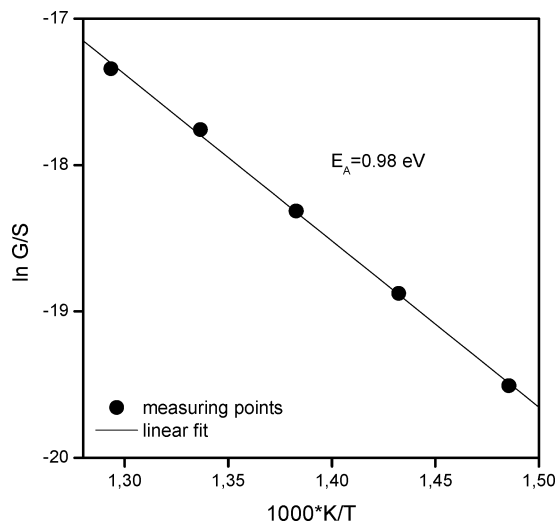


Figure 8. Arrhenius plot of the conductivity of material A.

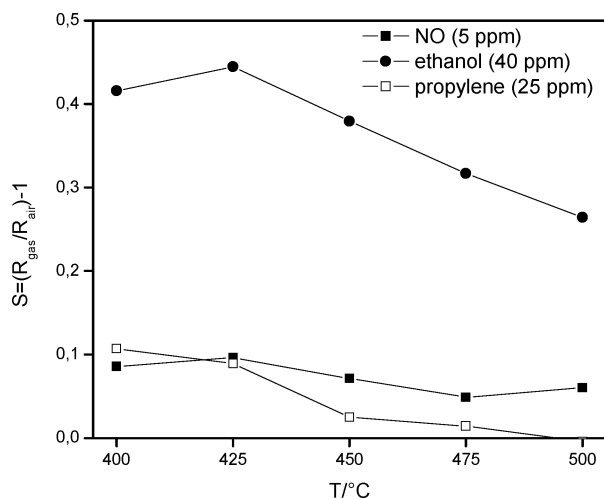


Figure 9. Temperature dependence of the sensitivity of material A.

increase of the resistance is observed; this is the typical behavior of p-type semiconductors. Additionally, as mentioned before, almost no cross sensitivity toward propylene could be found.

After these promising results, other Mo/Bi compounds prepared previously were tested for comparison and to see if they could serve as suitable precursors for the preparation of bismuthmolybdate single phases. A necessary condition for the application of the polyol method is a short-time (at least) stability of the Mo/Bi heterodinuclear arrangements against OH functions, and in this context the molybdenum/bismuth alkoxide complex **XXI** (Chart 2) recommended itself because it is stable, at least for short periods, in air. It, therefore, had been investigated in the past with respect to its behavior on silica surfaces.⁴¹

The use of **XXI** in the polyol method led to $\text{Bi}_2\text{Mo}_2\text{O}_9$ being found as the core product after calcinations, and Bi_2O_3 was found as a byproduct. Variation of the reaction parameters did not alter the process of product formation in favor

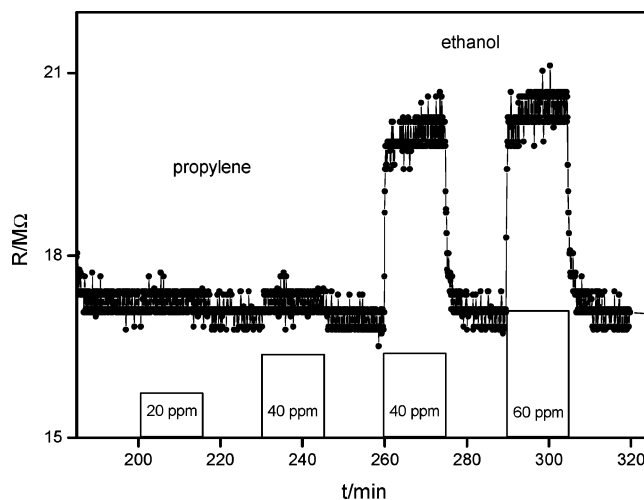
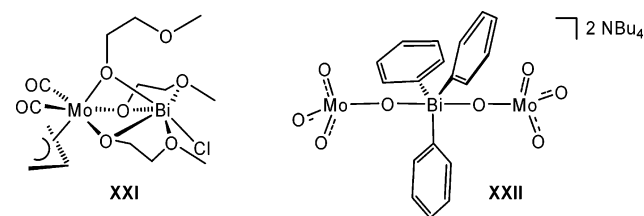


Figure 10. Response and recovery time of material A at $T = 500\text{ °C}$. The bars indicate the concentration steps of the admixed gases and the period of the test gas pulse, while the curve above shows the response of the resistance during the application of propylene and ethanol.

Chart 2



of a single-phase compound. Additionally, **XXII**, a molecular oxo complex^{2b} with a Mo/Bi ratio of 2:1 and with Bi in the oxidation state +V, was employed in the polyol method. Different preparations were performed with variation of hydrolyzing agent (H_2O , H_2O_2 , HNO_3), reaction time (1–5 h), and temperature (150–170 °C). All samples were calcined as described before. In all cases, monoclinic $\text{Bi}_2\text{Mo}_3\text{O}_{12}$ accompanied by MoO_3 was obtained. SEM pictures of materials obtained from both complexes revealed the formation of needles with a length in the micrometer to millimeter range. The outcome of this additional experiment thus shows that the relative molar ratio of Bi/Mo also determines the formation of different bismuth molybdate phases.

In the sensor-test measurements, a pronounced sensitivity toward the applied gases was not found in either case (materials derived from **XXI** or **XXII**); only a small sensitivity toward ethanol was noted.

Hence, promising results could be obtained only starting from **II**, but the polyol method so far seems to not be the ideal synthetic strategy to form *single-phase* nanoparticles from the complexes.

Conclusion

The reaction of $[\text{Cp}^*(\text{O})_2\text{Mo}-\text{O}-\text{Bi}(o\text{-tolyl})_2]_n$, **II**, with $\text{NBu}_4\text{OH}/\text{MeOH}$ intermediately leads to the species $(o\text{-tolyl})_2\text{BiOH}$ which polymerizes to give $[(o\text{-tolyl})_2\text{BiOH}]_n$, **1** ($\text{NBu}_4[\text{Cp}^*\text{MoO}_3]$ is formed as the byproduct). Compound **1** represents a rare example of a bismuthhydroxide compound, and it can be obtained in pure state from the reaction

(41) Limberg, C.; Hunger, M.; Habicht, W.; Kaifer, E. *Inorg. Chem.* **2002**, *41*, 3559.

of $[(o\text{-tolyl})_2Bi(\text{hmpa})_2]SO_3CF_3$ with NBu_4OH/H_2O in $thf/water$. Dissolved in dichloromethane, **1** immediately eliminates water to give $[(o\text{-tolyl})_2BiOBi(o\text{-tolyl})_2]$, **2**, which can be obtained on a preparative scale in this manner. If $[(o\text{-tolyl})_2Bi(\text{hmpa})_2]SO_3CF_3$ is reacted with $NBu_4OH/MeOH$ in dichloromethane, $(o\text{-tolyl})_2BiOH$ undergoes methanolysis before condensation leading to the isolation of $[(o\text{-tolyl})_2BiOMe]_n$, **3**. With molybdocene dihydrides, **II** reacts under the formation of $Mo-Bi$ bonds and $Mo-OH$ units, so that finally $[^R\text{Cp}_2\text{Mo(H)(Bi}(o\text{-tolyl})_2)]$, ($R = \text{Me}$ **4**, $R = \text{H}$ **5**) and $[\text{Cp}^*\text{Mo}_2\text{O}_5]$ are isolated as products. Compounds **4** and **5** can be obtained in pure state if **3** is chosen as the starting material to be reacted with the corresponding molybdocene dihydride, and it is noteworthy that **4** and **5** are the first representatives of this class of compounds that are isolable and thermodynamically stable. Unlike other molecular Mo/Bi compounds, **II** can be employed as precursor in the polyol method for the preparation of materials that exclusively contain bismuthmolybdates in form of nanoparticles and crystallites. These materials are biphasic and consist of $Bi_2Mo_2O_9$ and Bi_2MoO_6 , whose ratio can be determined by the choice of the hydrolyzing reagent. One of these materials proved to be capable of sensing $EtOH$ selectively at elevated temperatures.

In conclusion, molecular compounds containing $Mo-O-Bi$ moieties display interesting reactivities in the homoge-

neous phase that give access to novel compounds. Furthermore, they show promising properties as single-source precursors for bismuthmolybdates. Future research will have to reveal the most suitable method for their conversion to functional materials.

Acknowledgment. We are grateful to the Deutsche Forschungsgemeinschaft, the Fonds der Chemischen Industrie, the BMBF, and the Dr. Otto Röhm Gedächtnisstiftung for financial support. We also would like to thank P. Neubauer for crystal structure analyses and C. Jankowski for the preparation of starting materials. We further appreciate the contributions of D. Zornik to some of the experimental procedures reported here. M.S. gratefully acknowledges support by the Studienstiftung des Deutschen Volkes.

Supporting Information Available: X-ray crystallographic data in CIF format. This material is available free of charge via the Internet at <http://pubs.acs.org>. The crystallographic data (apart from structure factors) of **1**, **3**, and **4** were deposited at the Cambridge Crystallographic Data Centre as supplementary publications 607643, 607644, and 607645. Copies of the data can be ordered free of charge upon application to CCDC, 12 Union Road, Cambridge CB2 1EZ (Fax (+44)1223-336-033; e-mail deposit@ccdc.cam.ac.uk). IC061198C